China Geology 7 (2024) 248−263

China Geology

Journal homepage: http://chinageology.cgs.cn
https://www.sciencedirect.com/journal/china-geology

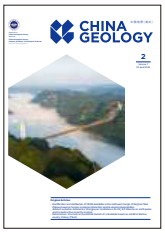

Analysis of debris flow control effect and hazard assessment in Xinqiao Gully, Wenchuan M_s 8.0 earthquake area based on numerical simulation

Chang Yang[a, b], Yong-bo Tie[b, c, d,*], Xian-zheng Zhang[b, c, d], Yan-feng Zhang[a], Zhi-jie Ning[a], Zong-liang Li[b, c, d]

[a] *Chinese Academy of Geological Sciences*, *Beijing* 100037, *China*
[b] *Chengdu Center of China Geological Survey*, *China Geological Survey*, *Chengdu* 610081, *China*
[c] *Technology innovation center for risk prevention and mitigation of geohazard*, *Ministry of Natural Resources*, *Chengdu* 611734, *China*
[d] *Observation and Research Station of Chengdu Geological Hazards*, *Ministry of Natural Resources*, *Chengdu* 610000, *China*

ARTICLE INFO

Article history:
Received 6 December 2023
Received in revised form 9 April 2024
Accepted 12 April 2024
Available online 25 April 2024

Keywords:
Landslide
Debris flow
Hazard assessment
Numerical simulation
OpenLISEM
Prevention and control project
Wenchuan M_s 8.0 earthquake
Xinqiao Gully
Sichuan province
Geological hazards survey engineering

ABSTRACT

Xinqiao Gully is located in the area of the 2008 Wenchuan M_s 8.0 earthquake in Sichuan province, China. Based on the investigation of the 2023 "6-26" Xinqiao Gully debris flow event, this study assessed the effectiveness of the debris flow control project and evaluated the debris flow hazards. Through field investigation and numerical simulation methods, the indicators of flow intensity reduction rate and storage capacity fullness were proposed to quantify the effectiveness of the engineering measures in the debris flow event. The simulation results show that the debris flow control project reduced the flow intensity by 41.05% to 64.61%. The storage capacity of the dam decreases gradually from upstream to the mouth of the gully, thus effectively intercepting and controlling the debris flow. By evaluating the debris flow of different recurrence intervals, further measures are recommended for managing debris flow events.

1. Introduction

On 12 May 2008, an earthquake measuring M_s 8.0 on the Richter scale occurred in the Wenchuan area of Sichuan Province, China, with a magnitude of 11 and seismic waves that circled the earth six times, affecting Thailand, Vietnam, and Pakistan. The earthquake severely damaged an area of more than 100×10^3 km^2, including 10 counties (cities) in the severely affected area, 41 counties (cities) in the moderately affected area, and 186 counties (cities) in the general disaster area. The earthquake killed 69227 people, injured 374643, and left 17923 missing, making it the most destructive earthquake since the founding of the People's Republic of China. Since then, landslides and mudslides have occurred frequently in the Wenchuan earthquake zone, continuing to cause loss of life and property in the area.

As a common geological disaster in mountainous regions, debris flows are famous for their sudden occurrence and high impacts (Iverson RM, 1997). Several significant debris flow events have resulted in substantial loss of life and economic damage in the Wenchuan area of Southwest China (Chen R et al., 2013; Zhang J et al., 2013; Ding MT and Huang T, 2019; Yin HQ et al., 2023). The giant debris flow events in Wenjia Gully (Ni HY et al., 2012) and Hongchun Gully (Ouyang CJ et al., 2015) resulted in severe river blockages and numerous casualties. According to statistics, the two events caused a total of 20 deaths and 66 missing persons and affected thousands of people. It is crucial to conduct prevention and disaster assessments of debris flow in mountainous areas.

Debris flow control involves two main aspects: Geotechnical engineering and biological engineering (Zhang WT et al., 2023). Geotechnical engineering includes disciplines such as blocking, protection, drainage, and crossing, which prevent soil erosion, stabilize slopes, and guide the flow (Chen X et al., 2015; Gong XL et al., 2021). Biological engineering is responsible for soil and water conservation, including agricultural and forestry soil and

First author: *E-mail address*: yangchang21@mails.ucas.ac.cn (Chang Yang).
* Corresponding author: *E-mail address*: tyongbo@mail.cgs.gov.cn (Tong-bo Tie).

Literary editor: Li-qiong Jia
doi:10.31035/cg2023144
2096-5192/© 2024 China Geology Editorial Office.

water conservation, as well as stabilizing material sources (Yang ZQ et al., 2013; Wang SY et al., 2017). Different measures are taken depending on the characteristics of the debris flow (Tang HM et al., 2019). A two-factor coupled assessment model, which considers the maximum flow depth and momentum, is usually used for zonal assessment of debris flow hazards (Ouyang CJ et al., 2019; Chang M et al., 2020; Cheng HL et al., 2022). This model can more accurately reflect the damage caused by debris flow impact and burial. Despite controls, failures and damage are common (Xiong MQ et al., 2016). Therefore, it is beneficial to evaluate the effectiveness of debris flow control measures and study the effectiveness of engineering solutions to enhance disaster prevention and control strategies.

Traditional research on debris flow control effects typically relies on qualitative analysis methods (Bai YJ et al., 2022; Tie YB et al., 2022). It involves summarising the characteristics and patterns of disasters through field investigations and experiments, analyzing the impact of prevention and control engineering on debris flows, and providing appropriate measures and recommendations (Haeberli W et al., 2001; Wang W et al., 2001; Imaizumi F et al., 2008; Tang C et al., 2011). However, qualitative analysis is primarily empirical and heavily influenced by human factors. To address this challenge, researchers have introduced mathematical assessment models, such as hierarchical analysis methods (Jun H et al., 2017), fuzzy mathematical methods (Fan JC et al., 2015; Li D et al., 2019), rough set theory (Pai PF et al., 2014; Li M et al., 2018), and neural network assessment models (Chang TC et al., 2010; Liu GX et al., 2013), and advanced research to a semi-quantitative stage. Nevertheless, qualitative and semi-quantitative analysis methods cannot accurately measure the specific impacts of control engineering on debris flow events, such as energy reduction and sediment interception. Consequently, quantitative analysis methods based on numerical simulation emerged.

Researchers have developed various numerical models with different assumptions. For instance, FLO-2D employs a single-block model suitable for simulating hydrodynamic-dominated dynamic processes (Nocentini M et al., 2015), while PFC, utilizing the discrete element method, is well-suited for grain flow simulations (Ray A et al., 2022). RAMMS has a depth-integral continuum model, making it suitable for simulating single-fluid models (Mikos M and Bezak N, 2021). In contrast, Massflow employed a generalized depth-integral model, primarily focusing on erosion dynamic processes (Horton AJ et al., 2019). OpenLISEM incorporates the contributions of viscous stress (Newtonian and non-Newtonian), virtual mass, generalized drag, and buoyancy in the solid-liquid two-phase fluid based on the generalized two-phase flow model, providing a broader range of physical significance compared to other models. OpenLISEM is utilized in regional debris flow hazards studies to offer quantitative information on the spatial and temporal distribution of flow velocity and depth (Pudasaini SP, 2012) and to analyze the dynamic processes. Through the above analyses, the results of the debris flow hazards assessment come out (Bastian VB et al., 2021).

The paper commences with an introduction to the geological conditions and environment of the study area, Xinqiao Gully. Data collection involves using remote sensing and ground investigation techniques to obtain essential information such as sediment grain size characteristics and traces of the bend super-high section. Subsequently, this data determines debris flow density, cross-section flow velocity, and depth. The OpenLISEM model is applied to analyze the Xinqiao Gully debris flow event. In addition, the model is inverted to assess the prevention and control effects. Two quantitative indexes, namely storage capacity fullness and flow intensity reduction rate of the dam, are proposed for the analysis. Finally, a two-factor model combining maximum flow depth and momentum is used to evaluate debris flow hazards at different recurrence intervals. The strategy presented in this paper aims to optimize control design and mitigate catastrophic risks.

2. Geological setting

The Xinqiao Gully is on the right bank of the Min River in Xinqiao Village, Weizhou Town, Wenchuan County, Sichuan Province, China (Fig. 1). The gully's outlet lies at 31°27′5.47″ N, 103°32′53.97″ E. The main channel flows through the culvert of the G213 and converges with the Min River, with Qipan Gully positioned about 800 m downstream. The gully comprises seven branch channels. Table 1 provides a detailed description of their topographic conditions. The main channel extends over a length of 4.92 km, covering a watershed area of 14.3 km^2. Various deposits, including flooding, collapse, landslide, and human-caused deposits, are found in the channel. Fig. 1 illustrates the implementation of prevention and control engineering measures following the Wenchuan earthquake to address the demand for disaster prevention.

The study area is in the Longmen Mountain fault zone, characterized by a complex geological structure. The maximum seismic acceleration in this region is 0.2 g, with a characteristic period of the seismic response spectrum at 0.3 s and an essential seismic intensity rated at VIII. The gully is on the upper plate of the Yingxiu fault and the Penguan anticlinorium's southern wing. The Penguan anticlinorium, located in Wenchuan, represents the largest anticlinorium, extending 100 km in length and 35 km in width, forming an uplift in the shape of a shuttle along the NE40º to 45º axial direction, covering Yinxin, Yingxiu, and Sanjiang. The Maowen Fault, Judging Mountain Fault, and Wuzhao Mountain Fault have impacted the southwestern region of the northern wing. In contrast, the northeastern section incorporates the Upper Sinian-Permian, and the southern wing

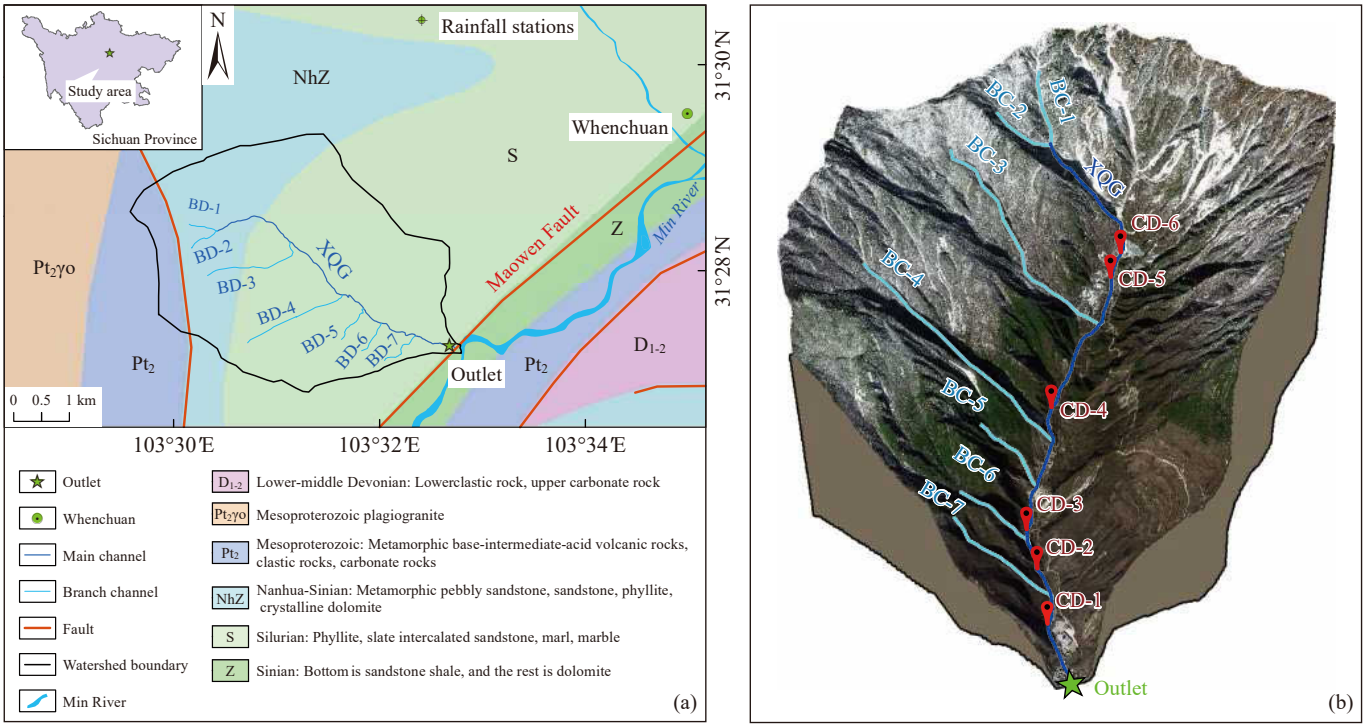

Fig. 1. Geological map (a) and topographic (b) map of the study area. BC–Branch Channel; CD–Check Dam.

Table 1. Topographic data in the Xinqiao Gully.

Gully	Channel length /km	Watershed area /km^2	Basin relief /m	Average gully gradien /‰
XQG	4.92	14.3	1192	225
BC-1	0.90	0.35	505	564
BC-2	0.72	0.24	430	598
BC-3	1.66	1.97	798	595
BC-4	1.74	1.68	1008	600
BC-5	0.73	0.29	591	859
BC-6	0.61	0.31	388	648
BC-7	0.75	0.19	531	716

Notes: XQG refers to Xinqiao Gully, and BC refers to Branch Channel.

is nearly bisected by the Yingxiu Fault.

The rock outcrops in the study area primarily comprise phyllite, sandstone, and limestone. In the Quaternary layer, various types of soil with varying thicknesses are observed in different areas. Upstream, steep slopes and hilltops are covered by a 1–2 m thick residual slope gravel soil. The midstream gentle slopes contain artificial landfill gravel soil with a 3–10 m thickness. The gully banks support a layer of floodplain sandy gravel soil measuring 1–4 m thick. The channel bed is encompassed by a 0.5–3 m thick layer of sandy gravel floodplain soil. Downstream slopes are characterized by silt-filled gravelly soil, with thicknesses ranging from 2 m to 5 m at the toe and foot. The accumulation area consists of floodplain and debris flow deposits, varying from 3 m to 15 m thicknesses.

Wenchuan is affected by the Pacific's warm high pressure in summer and the prevailing Northwest Plateau cold airflow in winter, resulting in two distinct natural climate zones. The valley area of Yingxiu and Xuankou districts south of Supaodian in Weizhou Town falls under the mountainous subtropical humid monsoon climate zone. In contrast, the valley area of Mianwu and Weizhou Towns north of Supaodian belongs to the warm-temperate continental semi-arid monsoon climate zone. The study area is in the semi-arid valley of the upper reaches of the Min River. The climate is dry with small and stable precipitation, with an annual measurement of 526.3 mm. Multi-year observations from nearby hydrological stations indicate that the 6-hour rainfall reached 53.3 mm, while the 1-hour rainfall reached 38.8 mm. The maximum daily precipitation in the area is 118.5 mm, with the highest 1-hour rainfall recorded at 42.2 mm and the maximum 10-minute rainfall at 11.5 mm.

The primary anthropogenic activities in the study area encompass farming and mining. The main residential area is downstream of the main ditch, near its confluence with the Minjiang River. On the other hand, the upstream branch ditch primarily serves as temporary housing for workers employed by Aba Mining Company. Site investigations indicate that farming activities are mainly concentrated near the residential area and have minimal impact on the surrounding vegetation. However, mining operations cause significant damage to vegetation, rock, and soil structures. The survey revealed that the slag produced during production was haphazardly piled in the trench, posing a high risk of debris flow disasters during heavy rainfall.

After investigation, the authors have gained preliminary knowledge of the historical mudslide events in this area. Before the Wenchuan earthquake, severe mudflows occurred in Xinqiao Gully in 1936, 1951, and 1998. Following the earthquake, the Department of Land and Resources of Sichuan Province conducted a post-earthquake geological

disaster emergency investigation and design project, resulting in the prompt engineering of the ditch. The design parameters for the blockage project are in Table 2, and the distribution is in Fig. 1. However, the earthquake disturbed the geotechnical body, weakening its structure and resulting in numerous avalanche-slip accumulations that converged at the bottom of the slope and in the ditch. These accumulations provided the necessary material for the formation of debris flows. After the earthquake, two debris flow events occurred on July 10, 2013, and June 26, 2023. The June 26, 2023 event, which the authors investigated, destroyed conduits and blockage of culverts on the 213 National Highway flowing into the Min River. Post-event analyses concluded that the event was caused by erosion of the upstream channel headwaters by storm surface runoff resulting from short-calendar duration heavy rainfall, as shown in Fig. 2.

3. Data and methods

Firstly, essential data is acquired through remote sensing interpretation, field investigation, and preliminary data organization. The parameters necessary for simulating the inversion of this debris flow event are determined through gradation tests, topographic analysis, image analysis, and empirical formulas. Following preprocessing, these parameters are input into the OpenLISEM model. Subsequently, the two-factor assessment model determines the hazard zoning situation under various recurrence intervals. The detailed process is illustrated in Fig. 3.

3.1. Data and sources

Table 3 presents the data used in this study for analyzing debris flow characteristics and simulating the runout processes. The data mainly include (1) digital surface model (DSM); (2) panchromatic image (PI); (3) digital elevation model (DEM); (4) satellite image (SI); (5) lithology and fault (SL&F) data; (6) field survey measurements.

3.2. Models and parameters

3.2.1. OpenLISEM model

OpenLISEM, an open-source hydrological software developed by the University of Twente in the Netherlands, is proficient in assessing debris flow hazards in mountainous or urban areas. It can simulate surface runoff, floods, high-sediment flow, and debris flow in catchment areas. The simulation provides results for various parameters, including flux, velocity, flow depth, solids thickness, outflow extent, and accumulation area (Van B et al., 2021). Furthermore, the OpenLISEM model can be employed for hazard zoning and to evaluate the impact of control engineering. It encompasses a debris flow model based on Pudasaini's generalized two-

Table 2. Control engineering information in the Xinqiao Gully.

Dam	Dam width/m	Dam height/m	Channel slope/‰	Deposition slope/‰	Design storage capacity/m^3	Storage of sedimentation /m^3
CD-1	33.5	3.5	123.0	86.0	3432.98	1142.44
CD-2	54.8	3.0	141.0	98.0	3991.43	3173.48
CD-3	21.6	3.5	176.3	123.2	2038.96	1977.64
CD-4	49.6	3.5	305.7	214.0	3006.38	2811.32
CD-5	48.6	4.5	222.0	147.0	4393.53	3506.90
CD-6	38.5	4.0	384.0	231.0	2013.07	2012.81

Notes: The data were obtained from field investigations. CD refers to Check Dam.

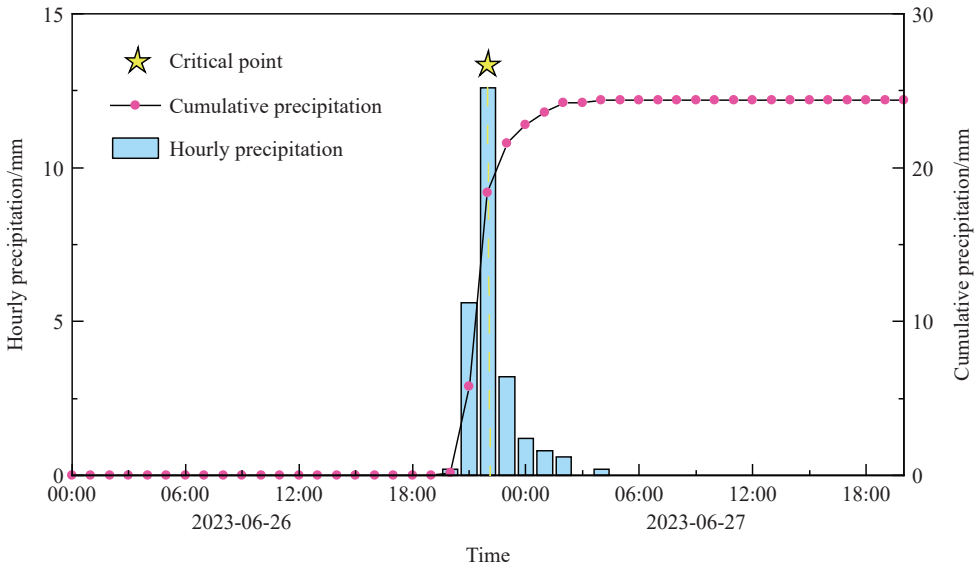

Fig. 2. Characteristics of trigging rainfall in the Xinqiao Gully.

phase flow model, allowing for a smooth transition between inviscid, high-sediment, and debris flow. The governing equations (Equs. 1–3) in OpenLISEM are as follows:

$$\frac{\partial h}{\partial t}+\frac{\partial (hu)}{\partial x}+\frac{\partial (hv)}{\partial y}=S \tag{1}$$

$$\frac{\partial (hu)}{\partial t}+\frac{\partial \left(hu^2\right)}{\partial x}+\frac{\partial (huv)}{\partial y}=S_x \tag{2}$$

$$\frac{\partial (hv)}{\partial t}+\frac{\partial \left(hv^2\right)}{\partial y}+\frac{\partial (huv)}{\partial x}=S_y \tag{3}$$

Where h is the flow depth, u and v are the flow velocities along the x and y directions, g is the gravity, S is the mass source, i.e., rainfall intensity minus infiltration intensity, S_x and S_y are the momentum sources, which are mainly generated by the action of volumetric and surface forces, the surface forces include the viscous force of the fluid, the friction between the solid phases, and the resistance between the two phases, and the volumetric force is mainly the gravitational force.

3.2.2. Simulation parameters

The elevation data in TIFF format were acquired through a DJ Mavic 3 UAV equipped with an RTK platform. The

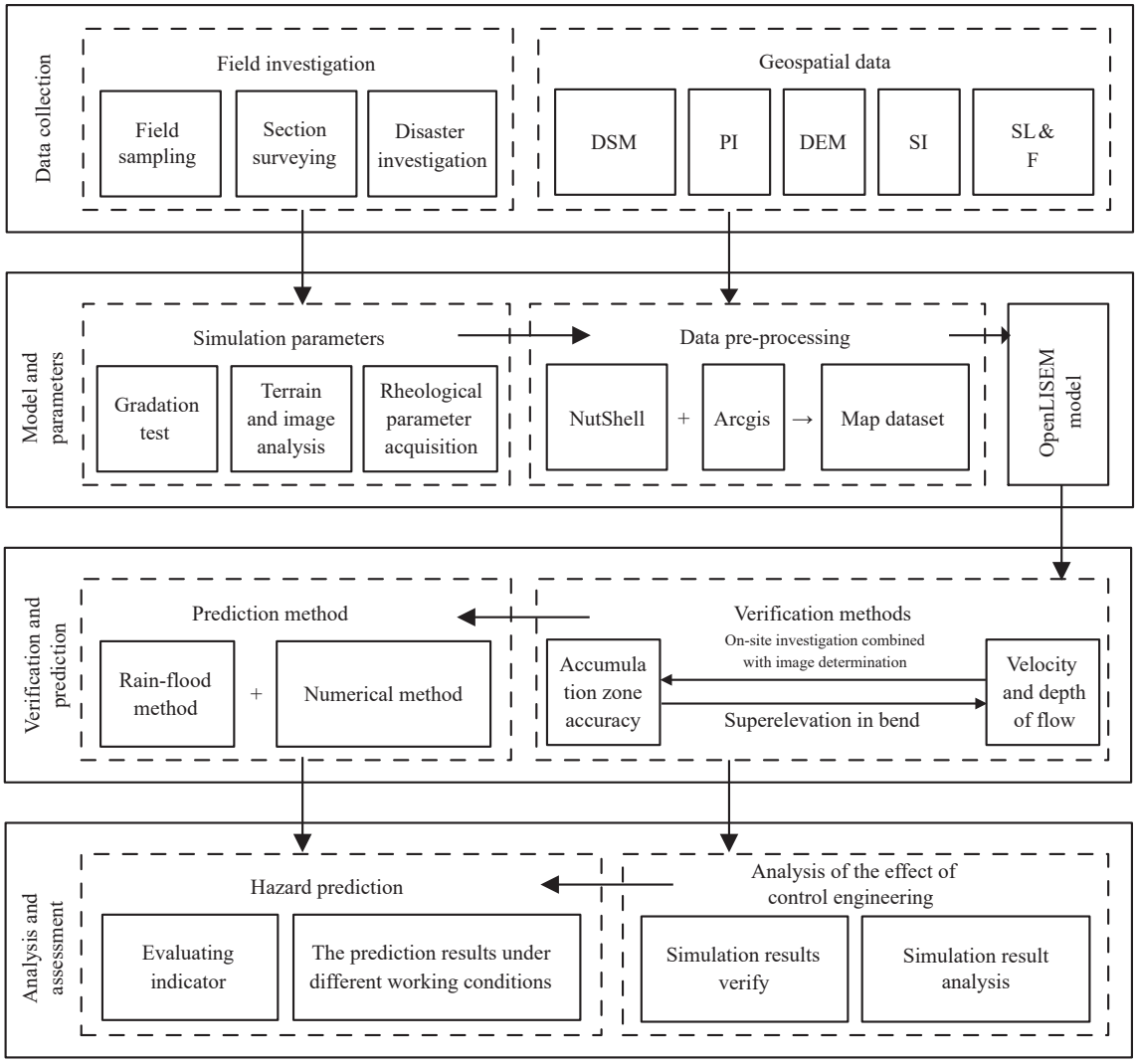

Fig. 3. Flow chart to analyze the preventive effect of the Xinqiao Gully debris flow and hazard assessment under different rainfall conditions.

Table 3. Data used and their sources in this study.

Name	Resolution	Source
Digital surface model	0.2 m	DJ Mavic 3 UAV equipped with an Real Time Kinematic (RTK) platform, Date: 2023.6.27
Panchromatic image	0.2 m	DJ Mavic 3 UAV equipped with an RTK platform, Date: 2023.6.27
Digital elevation model	12.5 m	ALOS (https://www.earthdata.nasa.gov/)
Satellite image	30.0 m	Geospatial Data Cloud (https://www.gscloud.cn/)
Lithology and fault	1∶50000	Chengdu Center of China Geological Survey

Note: DSM and PI data are available in the form of supplementary data.

parameters and terrain data in OpenLISEM were converted to MAP format using a Nutshell script, facilitating the batching process's automation. As per the study's requirements and to optimize computational efficiency, the grid cells in the simulation were resampled to a 2 m × 2 m resolution.

(i) Debris flow density

The sampling point was situated at the accumulation area, where the granulation curve was obtained through a gradation test, as illustrated in Fig. 4. Results revealed that the refined grains (less than 0.05 mm) constituted 10.28% of the total. The coarse grains (greater than 2.0 mm) accounted for 55.42 %, indicating that almost half of the debris flow in Xinqiao Gully consists of coarse-grained material. The debris flow density, calculated using the sediment-based method (Equ. 4) (Yu B, 2008), was determined to be 2.00 g/cm^3.

$$\gamma_d = P_{05}^{0.35} P_2 \gamma_v + \gamma_0 \tag{4}$$

Where P_{05} refers to the percentage content of refined grains with a particle size less than 0.05 mm expressed as a decimal, P_2 refers to the percentage content of coarse grains with a particle size greater than 2 mm expressed as a decimal, γ_v represents the characteristic density of the debris flow, and the value of which is taken as 2.00 g/cm^3, γ_0 is taken as 1.50 g/cm^3, which is the minimum density of the debris flow.

(ii) Total solid matter

Field investigations and topographic imagery analysis determined that approximately 42.2 × 10^3 m^3 of solid material was released during this debris flow event, primarily sourced from deposits behind the dam, in the channel, and accumulation areas. Despite an estimated total residual design capacity of approximately 18.9 × 10^3 m^3 for the dams based on design parameters and pre-debris event imagery, the post-dam deposition capacity identified in Table 2 was lower, around 14.6 × 10^3 m^3 due to the dam failure. Utilizing GIS tools, the analysis of solid volume deposited in the channel by the debris flow revealed a total of 21.9 × 10^3 m^3. The resulting deposited fan in the Xinqiao Gully debris flow event covered an area of approximately 4.72 × 10^3 m^2 with an average thickness of 1.2 m, estimating the volume of the deposited fan to be approximately 5.7 × 10^3 m^3, as depicted in Fig. 5.

(iii) Dynamic viscosity

In OpenLISEM, Pudasaini devised the rheological model for debris flow based on the analogy with Newtonian fluids (Pudasaini SP, 2012), which includes the solid concentration gradient (Equ. 5). The interaction between the solid and liquid phases during movement generates shear stress due to the concentration gradient, contributing to a more uniform distribution of concentration.

$$\tau^f = \eta^f \left[\nabla U^f + \left(U^f\right)^T - \eta_d \frac{A\left(\alpha^f\right)}{\alpha^f} [(\nabla \alpha^s)\left(U^f - U^s\right) + \left(U^f - U^s\right)(\nabla \alpha^s)] \right] \tag{5}$$

$$\eta_d = 0.278(\gamma_d - 1.20)^2 + 0.0035 \tag{6}$$

Where $A(\alpha^f)$ is the mobility of the fluid at the interface, η^f is the dynamic viscosity of the water, η_d is the dynamic

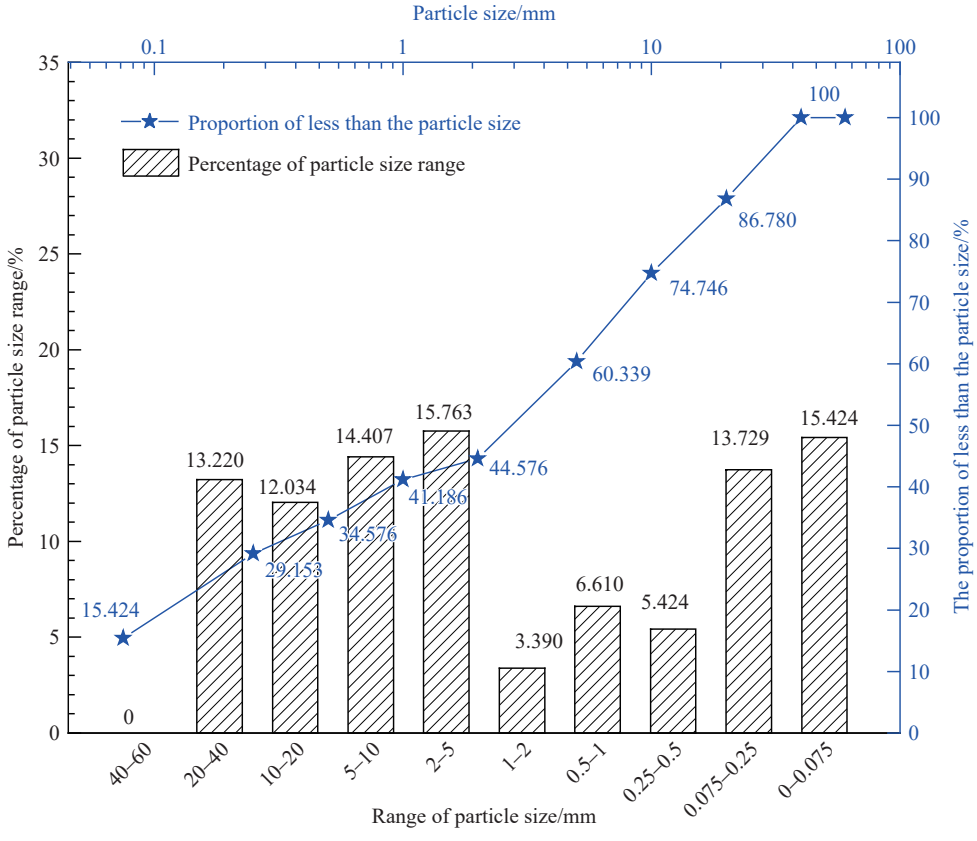

Fig. 4. Separation curves of debris flow sampling.

viscosity of the debris flow, and $\nabla\alpha^s$ is the solid concentration gradient. The dynamic viscosity was calculated using Equ. 6 to obtain. η_d is 0.18 Pa·s.

(iv) Peak discharge

Firstly, the authors calculated the rainstorm peak discharge at 20-year, 50-year, and 100-year recurrence using the reasoning formula method (Equ. 7). Then, the rain-flood method (Equ. 8) was employed for estimating the peak discharge of the debris flow (Cui P et al., 2011b). Following this, the volume of solid material during a debris flow event was determined using Equ. 9 and Equ. 10, the outcomes of which are detailed in Table 4.

$$Q_P = 0.278\Psi\frac{S}{\tau^n}F \tag{7}$$

$$Q_c = (1+\phi)Q_P D_c, \phi = (\gamma_c - \gamma_w)/(\gamma_h - \gamma_c) \tag{8}$$

$$Q = 0.264TQ_c \tag{9}$$

$$Q_H = Q(\gamma_c - \gamma_w)/(\gamma_h - \gamma_w) \tag{10}$$

Where Q_p is the rainstorm peak discharge (m^3/s), ψ is the peak runoff coefficient, s is the maximum one-hour rainfall (mm/h), τ is the confluence time (h), F is the catchment area (km^3), taken as 14.3, Q_c is the peak discharge of debris flow (m^3/s), Q is the total flow of a debris flow process (m^3), Q_H is the solid material wash-out volume of a debris flow event (m^3), D_c is the blocking coefficient, which is taken as 1.20 according to the field investigation results, γ_c is the density of debris flow (g/cm^3), calculated by Equ. 4 and taken as 2.00, γ_w is the density of clear water (g/cm^3), taken as 1.00, γ_h is the debris flow solid material density (g/cm^3), taken as 2.65, ϕ is the correction coefficient for the bulk weight of the debris-flow, which is calculated by Equ. 8 and taken as 1.54, T is the duration of debris flow (s), according to the survey, take

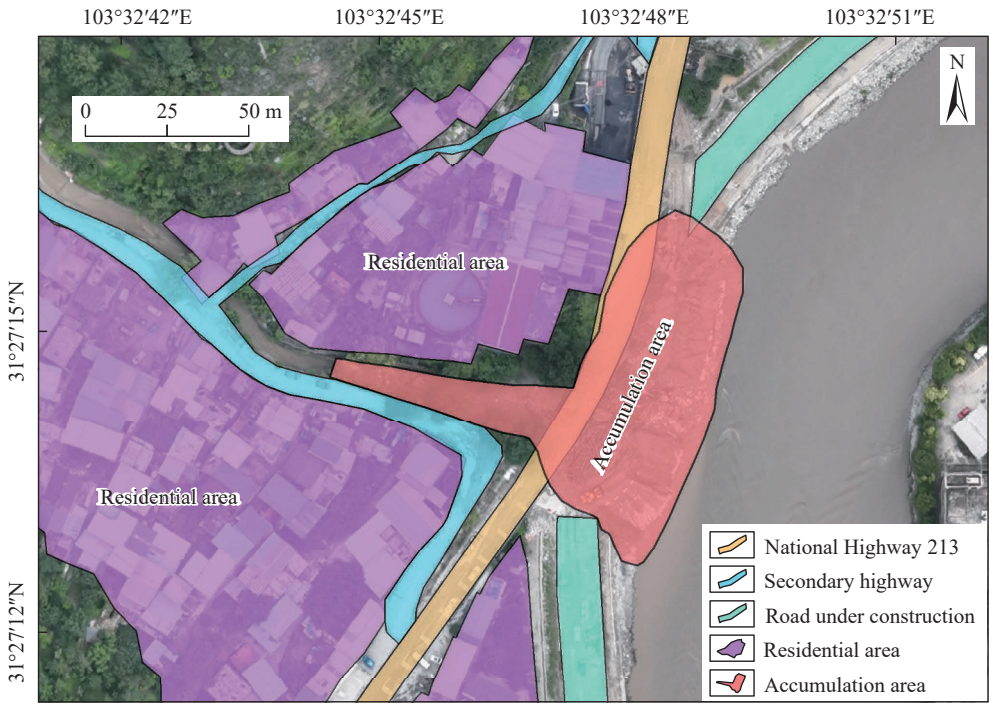

Fig. 5. Flow fan of the Xinqiao Gully debris.

Table 4. Results of the rain-flood method.

Recurrence P/%	Maximum one-hour rainfall s/(mm/h)	Confluence time τ /h	Peak runoff coefficient ψ	Rainstorm peak discharge Q_p /(m^3/s)	Debris flow peak discharge of Q_c/(m^3/s)	Total flow of a debris flow event Q/m^3	Solid material volume of a debris flow event Q_H/m^3
5	29.85	2.92	0.83	46.00	140.11	13.32	8.07
2	36.30	2.72	0.87	61.37	186.94	17.77	10.77
1	41.10	2.60	0.89	73.22	223.05	21.20	12.85

Table 5. Statistics of the results of the measured section.

No.	Sectional width B /m	Average flow depth h /m	centerline radius R_c /m	Superelevation Δh /m	angle of the channel θ_c	empirical correction factor C	Debris flow velocity V /(m/s)
1	5.68	3.27	41	1.64	0.24	5.85	4.39
2	6.06	3.15	46	1.90	0.27	4.16	5.72
3	5.78	2.92	49	2.05	0.20	4.36	6.19

3600.

3.3. Verification of simulation results

The accuracy of indicators such as the debris flow fan, flow velocity, flow depth, and run-out volume is often utilized for validation (Ding XY et al., 2023; Wang ZF et al., 2023). Flow velocity and depth are derived through inverse estimation utilizing the bend super-high section (Scheidl C et al., 2015), where the flow depth is estimated using the measured average flow depth, and the flow velocity is calculated using Equ. 11, with results detailed in Table 5. Moreover, the accuracy of the debris flow fan, Ad, is computed using Equ. 12, with a value range of [0,1], where a value closer to 1 indicates higher accuracy of the simulation results, and conversely, values nearing 0 denote less accurate simulation results. The run-out volume is estimated in section 3.2.2.

$$V = \sqrt{\frac{R_c g cos\theta_c \Delta h}{BC}}, C = 4.4^{2.46} \cdot \left(\frac{Bh}{R_{c\Delta h}}\right)^{1.46} \quad (11)$$

$$A_d = S_0^2 / (S_n \cdot S_m) \quad (12)$$

In Equ. 11, V is the velocity, g is the gravity, θ_c is the angle of the channel, C is the empirical correction factor, B is the channel width, R_c is the centerline radius, h is the average depth of flow, and Δh is the superelevation. In Equ. 12, A_d is the accuracy of the debris flow fan, S_0^2 is the area of overlap within the fan, S_n is the area of the numerically modeled fan, and S_m is the area of the field surveyed fan.

Field investigation and analysis of satellite images (Figs. 6a, b) identified the initiation zone in BC-1 and BC-2. The resulting debris flow followed the main channel, causing erosion. Figs. 6c–d illustrate the process of debris flow movement, primarily resulting in dam failure, road destruction, and siltation. The simulation of this event is centered on BC-1 and BC-2 as the initiation area.

Table 6 summarizes the simulated results (Fig.7) alongside the measured outcomes. The average relative errors for cross-section flow depth and flow velocity are 11.2 % and 8.5 %, respectively. The debris flow fan and run-out volume accuracy are reported at 70.2 % and 21.1 %, respectively. Notably, these errors stem from the debris flow's traversal of the National Highway 213 through a road culvert, which needs to be accounted for in the DEM, resulting in a discrepancy between the outlet and the actual terrain. Nevertheless, the simulation accuracy for flow depth and flow velocity in the investigated section remains high, effectively capturing the movement process of the Xinqiao Gully debris

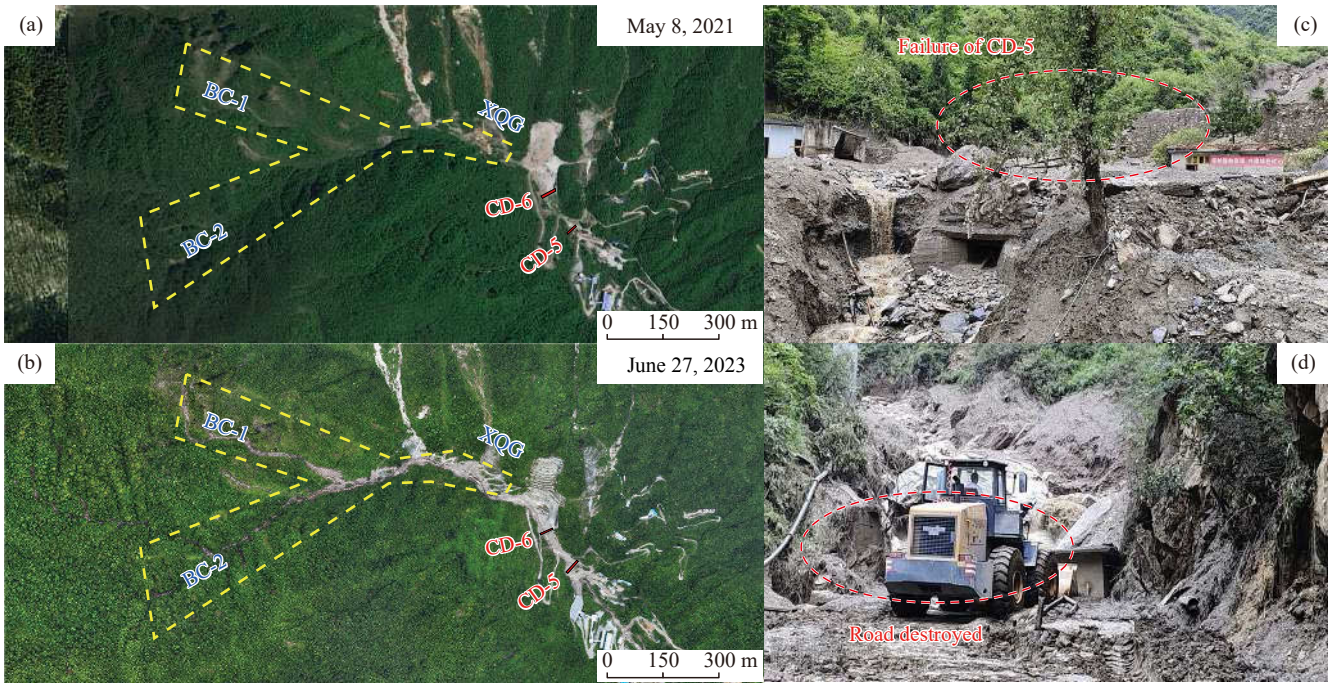

Fig. 6. Satellite images before (a) and after (b) the debris flow, and disaster characteristic map (c) and (d).

Table 6. Summary of verification methods.

Indicator	Measured values			Simulated values			Average relative errors /%	
flow depth /m	3.27	3.15	2.92	2.88	2.91	2.51	11.2	
flow velocity /(m/s)	4.39	5.72	6.19	4.62	4.95	5.77	8.5	
run-out volume /10^4m^3	0.57			0.69			21.1	
accuracy of the debris flow fan /%	area of the field surveyed fan /10^3m^3			area of the numerically modeled fan /10^3m^3			area of overlap within the fan	accuracy
	4.72			6.47			4.63	70.2

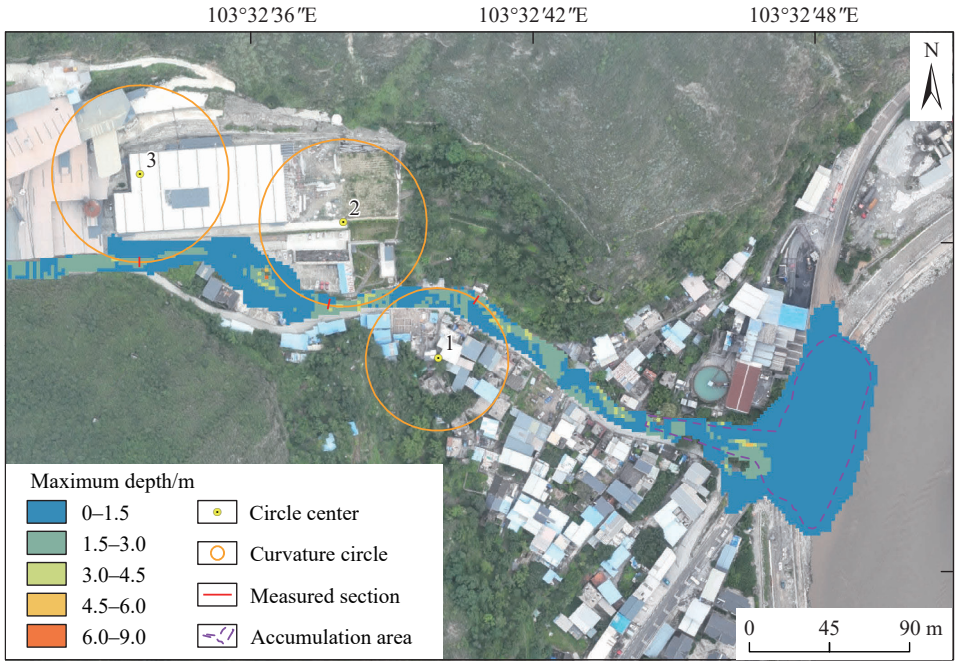

Fig. 7. Verification analysis of debris flow simulation. The numbers 1, 2 and 3 represent the measurement section numbers.

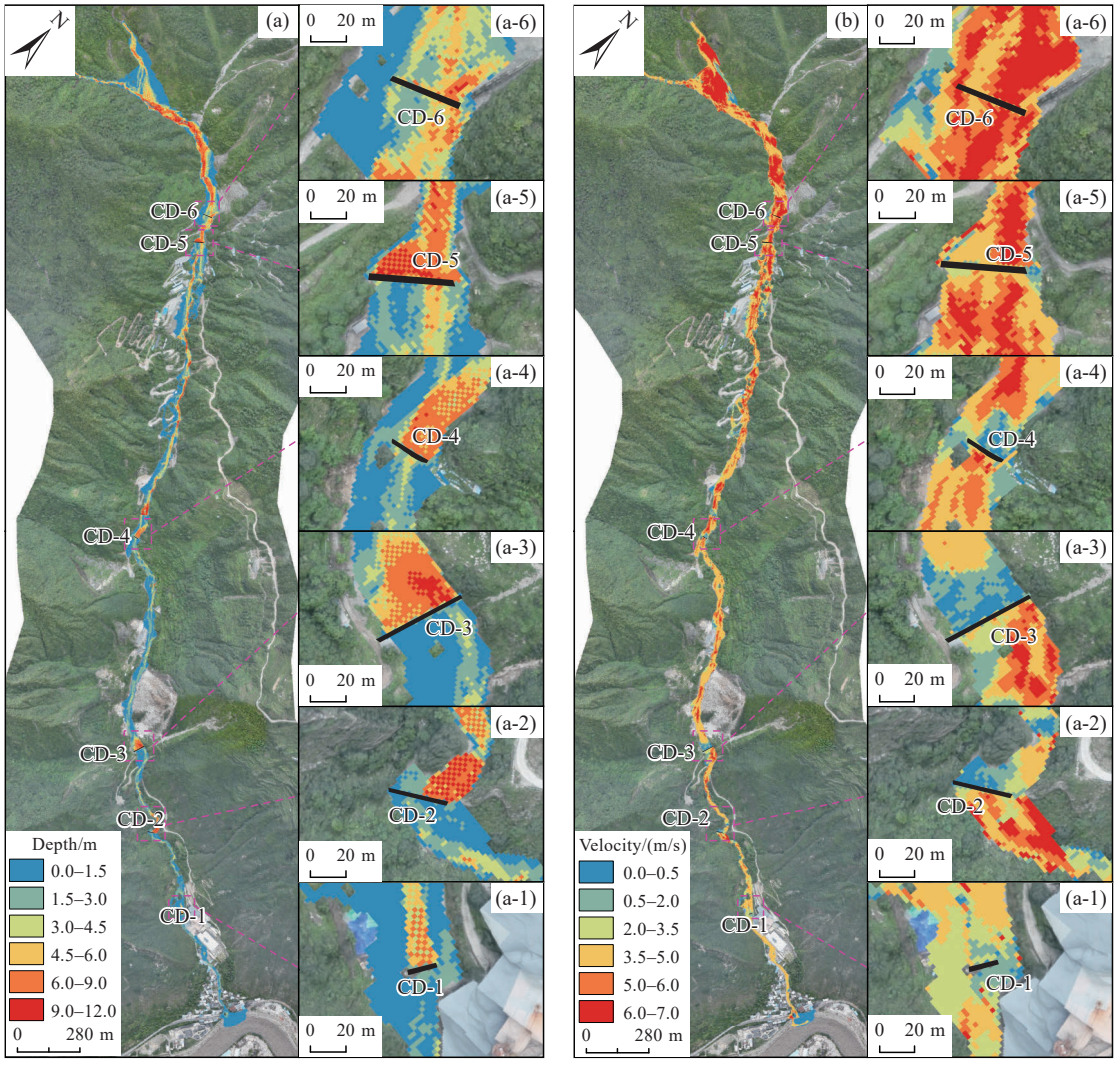

Fig. 8. Simulation results of the Xinqiao Gully debris flow. a–maximum depth; b–maximum velocity.

flow.

4. Control effectiveness analysis and debris flow hazard evaluation

4.1. Control effectiveness analysis

The results of the inversion of the Xinqiao Gully debris flow event are presented in Fig. 8. Figs. 8a–b depict the prominent post-dam siltation and pre-dam acceleration experienced after the debris flow passes through the check dam (Yang HQ et al., 2021). Post-dam siltation occurs as solid material accumulates behind a dam due to the interception of debris flow, leading to a significant increase in sediment depth compared to before the dam. On the other hand, pre-dam acceleration refers to the acceleration that follows the passage of a debris flow over a dam. This acceleration is attributed to the dam's obstruction of flow, resulting in the conversion of kinetic energy into gravitational potential energy (Chen Z et al., 2022). Once the potential energy reaches a certain threshold, it is transformed back into kinetic energy, leading to the acceleration of the flow. This paper proposes to employ the storage capacity fullness rate and flow intensity reduction rate as indices for assessing the impact of interception and energy reduction in dam projects. The indices are expressed as follows (Equs, 13, 14):

$$I_F = (HV_U \cdot HV_D) / HV_U \tag{13}$$

$$R = Q_A / Q_D \tag{14}$$

Where I_F is the flow intensity reduction rate, and the result is expressed as a % symbol, HV_U is the flow intensity upstream of the dam (m^2/s), HV_D is the flow intensity downstream of the dam (m^2/s), H is the flow depth (m), and V is the flow velocity (m/s). R is the dam's storage capacity fullness rate, Q_A is sedimentation storage, and Q_D is the design storage capacity.

The Table 7 summary reveals that the check dam achieves an average flow intensity reduction of 41.05% to 64.61%. Notably, CD-6 experiences a lower flow intensity reduction rate than other dams, potentially due to its proximity to the debris flow source and rapid burial during the debris flow initiation. Consequently, this dam's effectiveness in mitigating subsequent debris flows is limited, underscoring the impact of blockage when dams remain uncleared post-debris flow events. The storage capacity fullness rate of the check dam progressively decreases from the upstream to the mouth of the ditch, with CD-5 being an exception due to a localized failure, indicating successful interception and silting during the flow process. However, CD-2, situated near the residential area at the gully outlet, retains a high storage capacity fullness rate, suggesting a need for increased control of potential large-scale debris flows. It is important to note that the indicators proposed in this study aimed to quantify the control effectiveness on expected debris flows rather than after the event, in contrast to similar indicators such as the flow reduction rate. Analysis of hydro-meteorological data established the debris flow's recurrence period to be between 10 to 20 years, warranting detailed hazard analysis under more severe working conditions.

4.2. Indexes of debris flow hazard zoning

The hazard zoning of debris flows involves considering intensity and recurrence, as detailed in Tables 8, 9 (Ouyang CJ et al., 2015). Debris flow intensity is typically related to the flow's depth and impact force, generally expressed as a function of the flow intensity (Yan Y et al., 2023). Therefore, it is customary to utilize a two-factor model incorporating maximum flow depth and momentum coupling to classify the intensity of debris flows. These debris flow hazards are classified into various scenarios based on recurrence, including 20-year, 50-year, and 100-year cases.

4.3. Results of debris flow hazard assessment

The results of debris flow intensity zoning, based on Table 8, are visualized in Fig. 9. The red area, signifying high intensity, predominantly encompasses the inner part of the ditch, while the yellow area, indicating medium intensity, is concentrated on both sides of the nearby ditch. The green area, representing low intensity, is predominantly located in the upstream Aba Mining Company's building complex and the downstream accumulation area, situated away from the residential area near the ditch. Statistical findings (Table 10) indicate that as rainfall intensity rises, the area of high-intensity rainfall expands from 161.72 × 10^3 m^2 to 231.54 ×

Table 7. Calculated results of flow intensity reduction rate.

Dam	Flow intensity upstream of the dam HV_U /(m^2/s)	Flow intensity downstream of the dam HV_D /(m^2/s)	Flow intensity reduction rate I_F /%	Storage capacity fullness rate R /%
CD-1	10.81	4.31	60.13	33.28
CD-2	19.84	7.02	64.61	79.51
CD-3	10.60	6.25	41.05	96.99
CD-4	18.05	9.65	46.56	93.51
CD-5	39.03	15.09	61.33	79.82
CD-6	23.71	21.43	9.60	99.99

Table 8. Standards of debris flow intensity zoning.

Intensity	Depth h /m	Logic	Flow intensity hv /(m^2/s)
high	$h \geqslant 3.0$	∪	$hv \geqslant 8.0$
medium	$1.5 \leqslant h < 3.0$	∩	$2.0 \leqslant hv < 8.0$
low	$0.0 \leqslant h < 1.5$	∩	$0.0 \leqslant hv < 2.0$

Table 9. Hazard classification by intensity and probability of occurrence.

RecurrenceIntensity	[0,20)high	[20,50]medium	(50,100]low
high	high	high	medium
medium	high	medium	low
low	medium	low	low

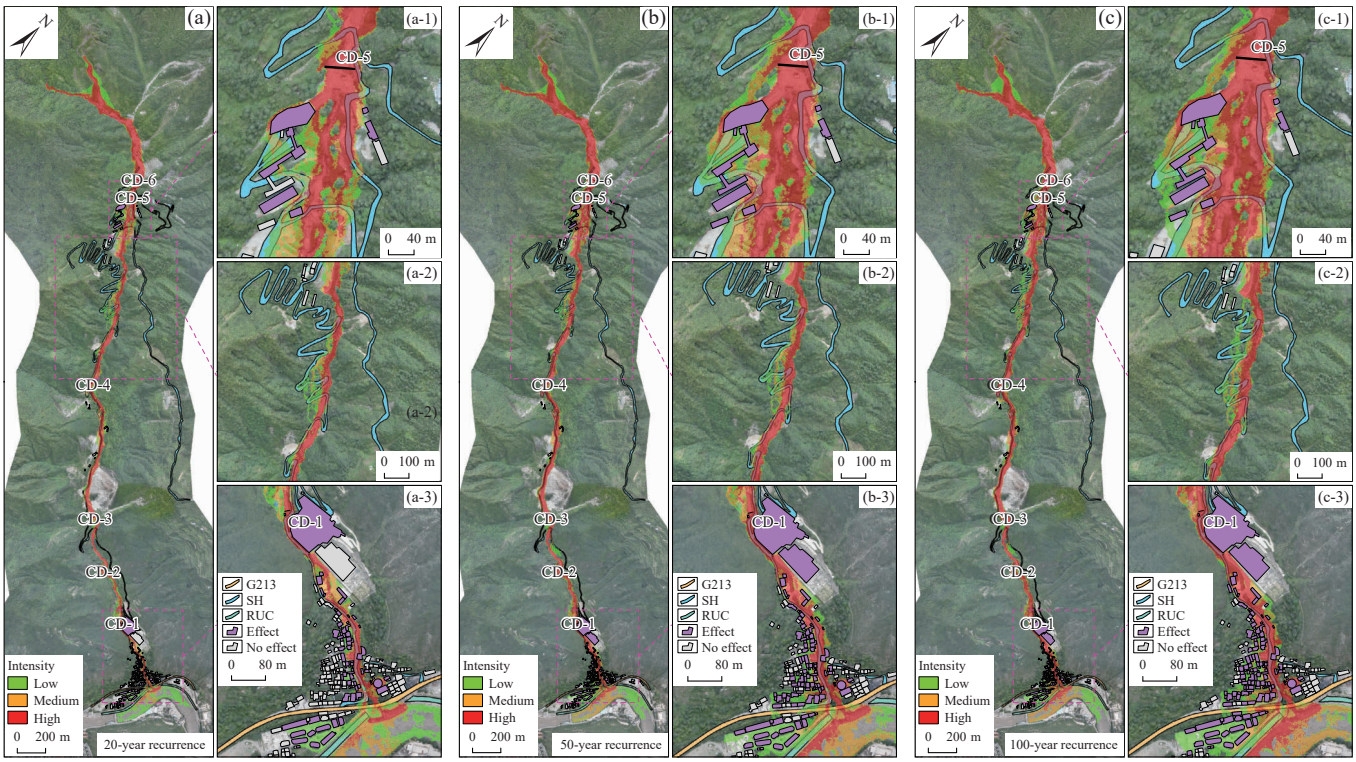

Fig. 9. Debris flow intensity zoning of different recurrence intervals. a–20-year recurrence interval; b–50-year recurrence interval; c–100-year recurrence interval. SH–Secondary highway; RUC–Road under construction.

Table 10. Areas classified as relatively low, medium, and high intensity.

Recurrence *P* /%	High-intensity area		Medium-intensity area		Low-intensity area	
	Area /10^3m^2	Proportion /%	Area /10^3m^2	Proportion /%	Area /10^3m^2	Proportion /%
5%	161.72	53.37	57.73	19.05	83.57	27.58
2%	204.70	56.40	72.83	20.07	85.39	23.53
1%	231.54	57.49	76.58	19.02	94.59	23.49

10^3 m^2, with its percentage increasing from 53.37 % to 57.49 %. Although the medium- and low-intensity rainfall areas similarly increase significantly, the percentage changes are negligible. The primary areas at risk include the ditches and banks.

Relying on the intensity of debris flow to delineate hazardous areas has limitations (Luna BQ et al., 2011). Combining intensity and occurrence probability levels (Table 9) is necessary to establish a hazard map of Xinqiao Gully debris flow. This process involves the utilization of three hazard grades: High, medium, and low (Fig. 10), overlaying the zoning situation of different recurrences. The high-hazard zone, which covers an area of 229.07×10^3 m^2, represents 56.67 % of the total threatened area and is primarily located in the fast and deep areas within the inner part of the ditch. The medium-hazard zone encompasses an area of 95.46×10^3 m^2, accounting for 23.62 % of the total threatened area, predominantly situated on either side of the ditch, with a fraction adjacent to the highway near the ditch bank. The low danger zone covers an area of 79.67×10^3 m^2, constituting 19.71 % of the total threatened area (Table 11), and is primarily situated in the accumulation area at the mouth of the ditch and on gently sloping terrain. Notably, the area of low-hazard zones for debris flow disasters with a 5% recurrence and the area of high-hazard zones for debris flow disasters with a 1% recurrence are both zero due to their infrequency.

The Xinqiao Gully debris flow exhibits consistent characteristics that can lead to disasters during various occurrences, primarily impacting the channel and its surrounding areas. It is crucial to closely monitor the construction area of the upstream Aba Mining Company and the residential area at the downstream gully mouth. Furthermore, debris flow in certain gully sections can result in road damage and siltation, hindering emergency investigations and rescue operations post-disaster. Additionally, with the intensification of rainfall, the high-hazard area for debris flow expands beyond the ditches, posing an increasing threat to residents living along the banks and highway facilities. To mitigate these risks, we propose improving the blocking project between CD-3 and CD-5 in the upstream section of the ditch. Moreover, raising the height of the downstream drainage channel and performing anti-blockage reconstruction on the culvert at the outlet of the G213 can help minimize the threat of debris flow to the safety of people's lives and public infrastructure.

5. Discussion

This study provides a practical approach for quantitatively evaluating the effectiveness of debris flow control projects in similar areas. The findings reveal a notable decrease in flow

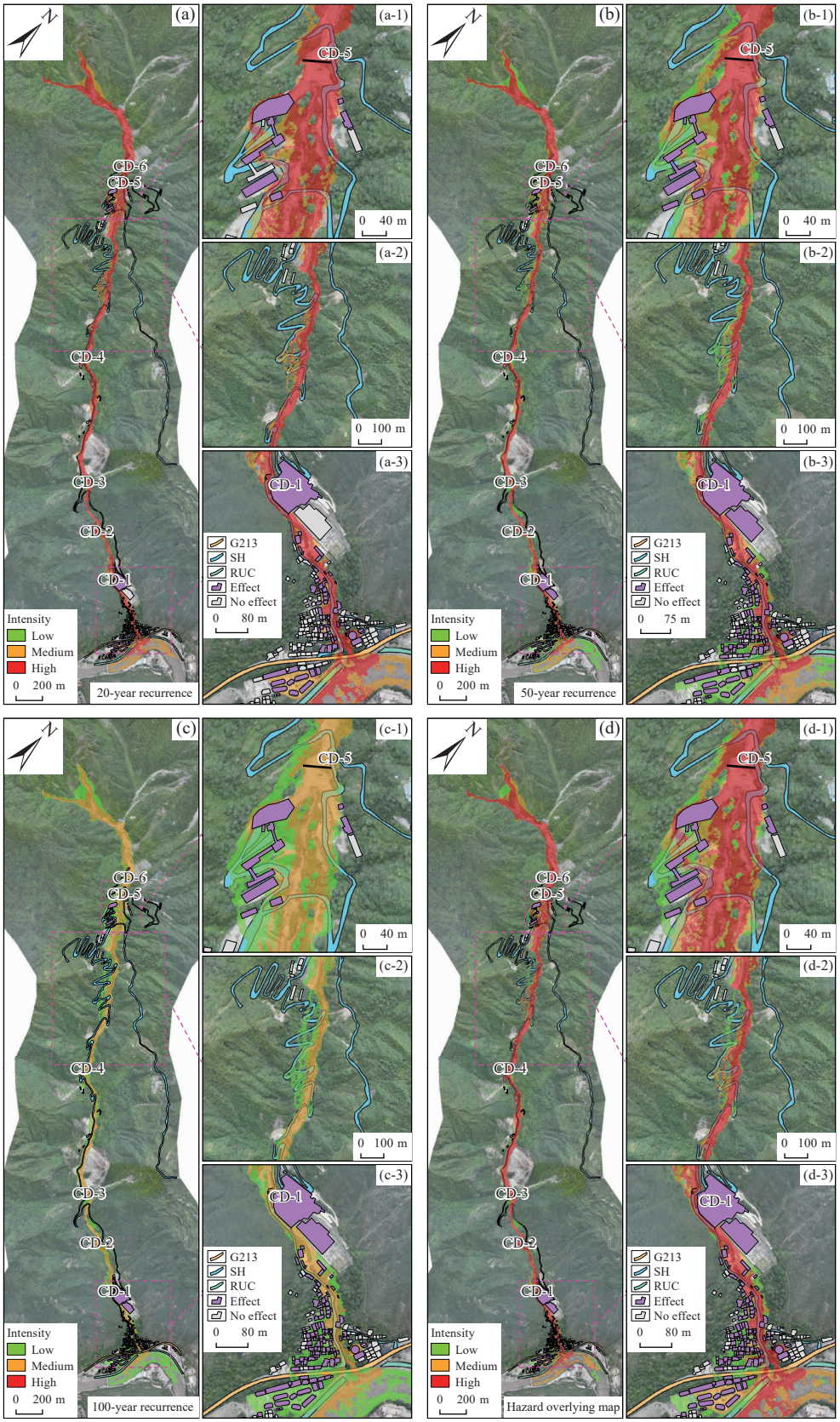

Fig. 10. Debris flow hazard zoning of different recurrence intervals. a–20-year recurrence interval; b–50-year recurrence interval; c–100-year recurrence interval; d–hazard overlying map.

intensity during the active phase of the Xinqiao Gully debris flow control project, affirming the effectiveness of the engineering measures. Furthermore, considering intensity and recurrence interval, the hazard zoning assessment offers a comprehensive understanding of the potential risks associated with debris flow in the region. Additionally, using the

Table 11. Areas classified as relatively low, medium, and high hazard.

Recurrence *P* /%	High-hazard area		Medium-hazard area		Low- hazard area	
	area /10^3m^2	proportion /%	area /10^3m^2	proportion /%	area /10^3m^2	proportion /%
5	219.45	72.42	83.57	27.58	0	0
2	204.70	56.40	72.83	20.07	85.39	23.53
1	0	0	231.54	57.49	171.18	42.51
overlying	229.07	56.67	95.46	23.62	79.67	19.71

OpenLISEM model for quantitative analysis highlights the vital importance of implementing effective control measures to mitigate the impact of debris flow on the region's livelihood and public infrastructure.

5.1. Applicability of the OpenLISEM Model

Debris flow can be categorized into slope debris flow and gully debris flow based on watershed geomorphology. The crucial factor for the numerical simulation of slope debris flow is determining the distribution of debris sources (Ni HY et al., 2014). In contrast, gully debris flow primarily involves identifying the position of drainage points and the flow discharge curve (Chang M et al., 2017). In the case of the Xinqiao Gully debris flow event, the initiation area, characterized by a short, indistinct valley form and high position, can be considered a process of slope erosion starts to form debris flow.

The OpenLISEM model has been extensively utilized for quantitative analysis and assessment of debris flow disasters (Van B et al., 2021). This study has demonstrated its effectiveness in simulating debris flow events and evaluating the impact of engineering control measures. However, it is important to recognize certain limitations and drawbacks of the model. As the current version lacks the function to set drainage points and flow discharge curves, OpenLISEM is unsuitable for gully debris flow and can be replaced by Flo-2D (Kurovskaia VA et al., 2022) and Massflow (Horton AJ et al., 2019) software. Despite providing valuable quantitative analysis capabilities, the accuracy and reliability of OpenLISEM may be influenced by factors such as setting simulation boundary conditions and grid accuracy. Therefore, future research should address these limitations by utilizing local grid refinement techniques.

5.2. Evaluation of Debris Flow Control Effectiveness

Previous studies evaluating the effectiveness of debris flow control have primarily relied on post-disaster qualitative or semi-quantitative analyses, overlooking the assessment of control measures (Tang C et al., 2011; Li M et al., 2018). Hence, this paper conducts a quantitative study on the effectiveness of debris flow control engineering, aiming to improve the understanding of the efficacy of engineering measures in mitigating debris flow hazards, which can, in turn, inform disaster emergency management. The results show that through the careful implementation of control engineering, the intensity of debris flow can be significantly reduced, consequently mitigating the activity intensity of debris flow and confirming the effectiveness of such measures in minimizing potential hazards.

5.3. Disaster prevention and mitigation recommendations

Mountain disaster prevention and control in southwest China boast a rich historical background (Cui P et al., 2003; Cui P et al., 2011a; Chen X et al., 2015a). Grounded in the three fundamental principles of prevention, control, and avoidance, a range of methods, including geotechnical engineering and bioengineering, are employed to establish systems focusing on preventing debris flow occurrence (SPDO), controlling debris flow movement (SCDM), and averting debris flow damage (SPDD) (Cui P et al., 2011a; Chen X et al., 2015). Specifically, the approach adopted in the Xinqiao Gully centers on SCDM, involving blocking engineering in the upper and middle gully sections and drainage engineering in the downstream accumulation area.

However, Current research indicates that under the most perilous conditions of the Xinqiao Gully debris flow, further optimization and enhancement of control measures are necessary to ensure effective mitigation of debris flow hazards. It is recommended to bolster solutions such as increasing interception projects and rebuilding drainage channels to address potential shortcomings and enhance disaster prevention and reduction capabilities. Moreover, future research could emphasize the development of comprehensive risk management strategies for debris flow events within the broader area. It may involve utilizing advanced modeling techniques, integrating real-time monitoring systems, and exploring innovative engineering solutions to fortify the region's safety and disaster resilience.

6. Conclusions

In general, secondary geological hazards such as landslides and debris flows will continue to occur for several years, decades, and even centuries after a mega-earthquake. These hazards cause secondary damage to the local population. Geologists have a responsibility to go deep into the disaster area to study the hazards and make management recommendations to reduce future losses.

In this study, investigating the debris flow event in the Xinqiao Gully involved a quantitative analysis of the effectiveness of debris flow control measures. The simulation obtains the distribution of maximum flow velocity and depth of debris flow with recurrence intervals of 20, 50, and 100 years to predict the debris flow disaster under different rainfall frequencies. Subsequently, the intensity and hazard zoning were determined for various rainfall frequencies. Finally, a hazard overlay map was generated utilizing a two-

factor evaluation model. The conclusions drawn from the research are as follows.

(i) Field investigation revealed that the source of the debris flow originates in areas BC-1 and BC-2, following the process of rainfall, confluence, initiation of runoff scour, debris flow, accumulation of blocked silt, overtopping, and movement along the ditch into the river.

(ii) The impact of control engineering on the debris flow process in this event was analyzed based on the OpenLISEM model and field investigation. It was suggested to utilize indicators such as the rate of reduction in flow intensity and the rate of fullness of the dam's storage capacity for measuring the impact of control engineering. The results show a decrease in Xinqiao Gully debris flow intensity ranging from 41.05 % to 64.61 %, with the storage capacity of dams decreasing from the upstream to the outlet. It suggests successful interception of debris flow and prevention of siltation during the movement process. However, it is essential to ensure timely removal of sediment buildup behind the dam.

(iii) The two-factor model was utilized to evaluate the hazard of debris flow zoning. Findings revealed that the high-hazard area is concentrated in the ditch channel, while the medium-hazard area is located on both sides. The low-hazard area is primarily situated in the construction area of Aba Mining Company and the residential area downstream of the ditch mouth. It was noted that as rainfall intensity increases, the hazardous area expands to the surrounding areas.

(iv) Based on investigation and simulation prediction analysis, increasing the height of the CD-5 and CD-6 dams upstream and constructing additional barriers between the CD-3 and CD-5 is recommended. Moreover, consider increasing the height or width of the drainage ditch or installing additional barrier structures for roads or residential areas near the ditch.

CRediT authorship contribution statement

All authors contributed to the study. Material preparation, data collection, and analysis were conducted by Chang Yang, Yan-feng Zhang, and Xian-zheng Zhang, with Chang Yang completing the photographs and tables. The initial draft of the manuscript was authored by Chang Yang, Yong-bo Tie, and Zong-liang Li, with all authors contributing to the manuscript's revision. Zhi-jie Ning participated in the field investigation, and all authors reviewed and approved the final draft.

Declaration of competing interest

The authors declare no conflicts of interest.

Acknowledgment

This work is supported by the project of the China Geological Survey (No. DD20221746) and the National Natural Science Foundation of China (Grant Nos. 41101086). Thanks to researcher Ming-hui Li of the Chengdu Center of China Geological Survey for assistance in this study.

Data availability statement

The data underlying this article are available in the article and its online supplementary material (https://pan.baidu.com/s/19YneVK-tEH_EKJwOKGaz5Q, code: 7zn6).

References

Bai YJ, Tie YB, Meng MJ, Xiong XH, Gao YC, Ge H, Ba R, Xu W. 2022. Characteristics and temporal-spatial distribution of geohazards in western Sichuan. Sedimentary Geology and Tethyan Geology, 42(4), 666–674 (in Chinese with English abstract).

Bastian VB, Theo VA, Wei H, Tang C, Mavrouli O, Jetten VG, Van CJ. 2021. Towards a model for structured mass movements: The OpenLISEM hazard model 2.0a. Geoscientific Model Development, 14(4), 1841–1864. doi: 10.5194/gmd-14-1841-2021.

Chang M, Liu Y, Zhou C, Che HX. 2020. Hazard assessment of a catastrophic mine waste debris flow of Hou Gully, Shimian, China. Engineering Geology, 275, 105733. doi: 10.1016/j.enggeo.2020.105733.

Chang M, Tang C, Van AT, Cai F. 2017. Hazard assessment of debris flows in the Wenchuan earthquake-stricken area, South West China. Landslides, 14(5), 1783–1792. doi: 10.1007/s10346-017-0824-9.

Chang TC, Wang ZY, Chien YH. 2010. Hazard assessment model for debris flow prediction. Environmental Earth Sciences, 60(8), 1619–1630. doi: 10.1007/s12665-009-0296-x.

Chen R, Liu X, Huang E, Guo Z. 2013. Numerical analysis of emergency river restoration scheme for Qingping mega debris flow. Journal of Mountain Science, 10(1), 130–136. doi: 10.1007/s11629-013-2120-z.

Chen X, Cui P, You Y, Chen JG, Li DJ. 2015. Engineering measures for debris flow hazard mitigation in the Wenchuan earthquake area. Engineering Geology, 194, 73–85. doi: 10.1016/j.enggeo.2014.10.002.

Chen Z, He SM, Shen W, Wang DP. 2022. Effects of defense-structure system for bridge piers on two-phase debris flow wakes. Acta Geotechnica, 17(5), 1645–1665. doi: 10.1007/s11440-021-01296-5.

Cheng HL, Huang Y, Zhang WJ, Xu Q. 2022. Physical process-based runout modeling and hazard assessment of catastrophic debris flow using SPH incorporated with ArcGIS: A case study of the Hongchun gully. Catena, 212, 106052. doi: 10.1016/j.catena.2022.106052.

Cui P, Chen XQ, Zhu YY, Su FH, Wei FQ, Han YS, Liu HJ, Zhuang JQ. 2011a. The Wenchuan Earthquake (May 12, 2008), Sichuan Province, China, and resulting geohazards. Natural Hazards, 56(1), 19–36. doi: 10.1007/s11069-009-9392-1.

Cui P, Hu KH, Zhuang JQ, Yang Y, Zhang JQ. 2011b. Prediction of debris-flow danger area by combining hydrological and inundation simulation methods. Journal of Mountain Science, 8(1), 1–9. doi: 10.1007/s11629-011-2040-8.

Cui P, Liu SQ, Tang BX, Chen XQ. 2003. Debris flow prevention pattern in national parks - Taking the world natural heritage Jiuzhaigou as an example. Science in China E:Technological Sciences, 46(7), 1–11. doi: 10.1360/03ez0004.

Ding MT, Huang T. 2019. Vulnerability assessment of population in mountain settlements exposed to debris flow: A case study on Qipan gully, Wenchuan County, China. Natural Hazards, 99(1), 553–569.

doi: 10.1007/s11069-019-03759-1.

Ding XY, Hu WJ, Liu F, Yang X. 2023. Risk assessment of debris flow disaster in mountainous area of northern Yunnan province based on FLO-2D under the influence of extreme rainfall. Frontiers in Environmental Science, 11, 1252206. doi: 10.3389/fenvs.2023.1252206.

Fan JC, Huang HY, Liu Chang, Yang CL, Guo JJ, Chang CF, Chang YC. 2015. Effects of landslide and other physiographic factors on the occurrence probability of debris flows in central Taiwan. Environmental Earth Sciences, 74(2), 1785–1801. doi: 10.1007/s12665-015-4187-z.

Gong XL, Chen XQ, Chen KT, Zhao WY, Chen JG. 2021. Engineering planning method and control modes for debris flow disasters in scenic areas. Frontiers in Earth Science, 9, 712403. doi: 10.3389/feart.2021.712403.

Haeberli W, Kääb A, Mühll DV, Teysseire P. 2001. Prevention of outburst floods from periglacial lakes at Grubengletscher, Valais, Swiss Alps. Journal of Glaciology, 47(156), 111–122. doi: 10.3189/172756501781832575.

Horton AJ, Hales TC, Ouyang CJ, Fan XM. 2019. Identifying post-earthquake debris flow hazard using Massflow. Engineering Geology, 258, 105134. doi: 10.1016/j.enggeo.2019.05.011.

Imaizumi F, Sidle RC, Kamei R. 2008. Effects of forest harvesting on the occurrence of landslides and debris flows in steep terrain of central Japan. Earth Surface Processes and Landforms:The Journal of the British Geomorphological Research Group, 33(6), 827–840. doi: 10.1002/esp.1574.

Iverson RM. 1997. The physics of debris flows. Reviews of Geophysics, 35(3), 245–296. doi: 10.1029/97rg00426.

Jun H, Min DH, Yoon HK. 2017. Determination of monitoring systems and installation location to prevent debris flow through web-based database and AHP. Marine Georesources & Geotechnology, 35(8), 1049–1057. doi: 10.1080/1064119x.2017.1280716.

Kurovskaia VA, Chernomorets SS, Krylenko IN, Vinogradova TA, Dokukin MD, Zaporozhchenko EV. 2022. Buzulgan rockslide: Simulation of debris flows along Gerkhozhan-Su river and scenarios of their impact on Tyrnyauz Town after Changes in 2020. Water Resources, 49(1), 58–68. doi: 10.1134/s0097807822010110.

Li D, Zhang HQ, Li YQ, Zhen Z, Bu SL, Tang XC, Chen S, Luo S, Tian SF, Xiong MM. 2019. Hazard assessment of debris flow in Guangxi, China based on hydrodynamics mechanism. Environmental Earth Sciences, 78(2), 1–17. doi: 10.1007/s12665-018-8040-z.

Li M, Tian CS, Wang YK, Liu Q, Lu YF, Wang S. 2018. Impacts of future climate change (2030–2059) on debris flow hazard: A case study in the Upper Minjiang River basin, China. Journal of Mountain Science, 15(8), 1836–1850. doi: 10.1007/s11629-017-4787-z.

Liu GX, Dai E, Ge QS, Wu WX, Xu XC. 2013. A similarity-based quantitative model for assessing regional debris-flow hazard. Natural Hazards, 69(1), 295–310. doi: 10.1007/s11069-013-0709-8.

Luna BQ, Blahut J, Van CJ, Sterlacchini S, Van TW, Akbas SO. 2011. The application of numerical debris flow modelling for the generation of physical vulnerability curves. Natural Hazards and Earth System Sciences, 11(7), 2047–2060. doi: 10.5194/nhess-11-2047-2011.

Mikos M, Bezak N. 2021. Debris Flow Modelling Using RAMMS Model in the Alpine Environment With Focus on the Model Parameters and Main Characteristics. Frontiers in Earth Science, 8, 605061. doi: 10.3389/feart.2020.605061.

Ni HY, Zheng WM, Song Z, Xu W. 2014. Catastrophic debris flows triggered by a 4 July 2013 rainfall in Shimian, SW China: formation mechanism, disaster characteristics and the lessons learned. Landslides, 11(5), 909–921. doi: 10.1007/s10346-014-0514-9.

Ni HY, Zheng WM, Tie YB, Su PC, Tang YQ, Xu RG, Wang DW, Chen XY. 2012. Formation and characteristics of post-earthquake debris flow: a case study from Wenjia gully in Mianzhu, Sichuan, SW China. Natural Hazards, 61(2), 317–335. doi: 10.1007/s11069-011-9914-5.

Nocentini M, Tofani V, Gigli G, Fidolini F, Casagli N. 2015. Modeling debris flows in volcanic terrains for hazard mapping: the case study of Ischia Island (Italy). Landslides, 12(5), 831–846. doi: 10.1007/s10346-014-0524-7.

Ouyang CJ, He SM, Tang C. 2015. Numerical analysis of dynamics of debris flow over erodible beds in Wenchuan earthquake-induced area. Engineering Geology, 194, 62–72. doi: 10.1016/j.enggeo.2014.07.012.

Ouyang CJ, Wang ZW, An HC, Liu XR, Wang DP. 2019. An example of a hazard and risk assessment for debris flows-A case study of Niwan Gully, Wudu, China. Engineering Geology, 263, 105351. doi: 10.1016/j.enggeo.2019.105351.

Pai PF, Li LL, Hung WZ, Lin KP. 2014. Using ADABOOST and Rough Set Theory for Predicting Debris Flow Disaster. Water Resources Management, 28(4), 1143–1155. doi: 10.1007/s11269-014-0548-8.

Pudasaini SP. 2012. A general two-phase debris flow model. Journal of Geophysical Research: Earth Surface, 117, F3. doi: 10.1029/2011jf002186.

Ray A, Verma H, Bharati AK, Rai R, Koner R, Singh TN. 2022. Numerical modelling of rheological properties of landslide debris. Natural Hazards, 110(3), 2303–2327. doi: 10.1007/s11069-021-05038-4.

Scheidl C, McArdell BW, Rickenmann D. 2015. Debris-flow velocities and superelevation in a curved laboratory channel. Canadian Geotechnical Journal, 52(3), 305–317. doi: 10.1139/cgj-2014-0081.

Tang C, Zhu J, Ding J, Cui XF, Chen L, Zhang JS. 2011. Catastrophic debris flows triggered by a 14 August 2010 rainfall at the epicenter of the Wenchuan earthquake. Landslides, 8(4), 485–497. doi: 10.1007/s10346-011-0269-5.

Tang HM, Wasowski J, Juang CH. 2019. Geohazards in the three Gorges Reservoir Area, China Lessons learned from decades of research. Engineering Geology, 261, 105267. doi: 10.1016/j.enggeo.2019.105267.

Tie YB, Ge H, Gao YC, Bai YJ, Xu W, Gong LF, Wang JZ, Tian K, Xiong XH, Fan WL, Zhang XZ. 2022. The research progress and prospect of geological hazards in Southwest China since the 20th Century. Sedimentary Geology and Tethyan Geology, 42(4), 653–665 (in Chinese with English abstract).

Van B, Lombardo LG, Ma CY, Van C, Jetten V. 2021. Physically-based catchment-scale prediction of slope failure volume and geometry. Engineering Geology, 284, 105942. doi: 10.1016/j.enggeo.2020.105942.

Wang SY, Meng XM, Chen G, Guo P, Xiong MQ, Zeng RQ. 2017. Effects of vegetation on debris flow mitigation: A case study from Gansu province, China. Geomorphology, 282, 64–73. doi: 10.1016/j.geomorph.2016.12.024.

Wang W, Xu WL, Liu SJ. 2001. Prevention of debris flow disasters on Chengdu-Kunming Railway. Journal of Environmental Sciences, 13(3), 333–336.

Wang ZF, Zhang XS, Zhang XZ, Wu MT, Wu B. 2023. Hazard assessment of potential debris flow: A case study of Shaling Gully,

Lingshou County, Hebei Province, China. Frontiers in Earth Science, 11, 1089510. doi: 10.3389/feart.2023.1089510.

Xiong MQ, Meng XM, Wang SY, Guo P, Li YJ, Chen G, Qing F, Cui ZJ, Zhao Y. 2016. Effectiveness of debris flow mitigation strategies in mountainous regions. Progress in Physical Geography, 40(6), 768–793. doi: 10.1177/0309133316655304.

Yan Y, Tang H, Hu KH, Turowski JM, Wei FQ. 2023. Deriving Debris-Flow Dynamics From Real-Time Impact-Force Measurements. Journal of Geophysical Research:Earth Surface, 128(3), e2022JF006715. doi: 10.1029/2022jf006715.

Yang HQ, Haque ME, Song KL. 2021. Experimental study on the effects of physical conditions on the interaction between debris flow and baffles. Physics of Fluids, 33(5), 056601. doi: 10.1063/5.0046670.

Yang ZQ, Liao LP, Jin H. 2013. Debris flows in the NiuQuan valley-the epicentre of Wenchuan Earthquake. Disaster Advances, 6, 393–403.

Yin HQ, Zhou W, Peng ZQ. 2023. Numerical simulation of rainfall-induced debris flow in the Hongchun gully based on the coupling of the LHT model and the Pudasaini model. Natural Hazards, 117(3), 2553–2572. doi: 10.1007/s11069-023-05956-5.

Yu B. 2008. Research on the Calculating Density by the Deposit of Debris Flows. Acta Sedimentologica Sinica, 26(5), 789–796 (in Chinese with English abstract).

Zhang J, Guo ZX, Cao SY, Singh VP. 2013. Scale model for the confluent area of debris flow and main river: a case study of the Wenjia Gully. Natural Hazards and Earth System Sciences, 13(12), 3083–3093. doi: 10.5194/nhess-13-3083-2013.

Zhang WT, Liu JF, Li DL, You Y, Yang HQ. 2023. Evaluation of comprehensive treatment effect of geotechnical and ecological engineering for debris flow: case of Wenchuan County, Sichuan Province. Natural Hazards, 116(1), 769–794. doi: 10.1007/s11069-022-05698-w.